




Article

Fabrication of Novel Hemp Charcoal Nanofiber Membrane for Effectual Adsorption of Heavy Metal Ions from Wastewater

Sana Ullah ^{1,2,†} , Osamu Ohsawa ^{1,†}, Tehmeena Ishaq ³, Motahira Hashmi ¹, Muhammad Nauman Sarwar ¹, Chunhong Zhu ⁴ , Yan Ge ⁵, Yeonju Jang ⁶ and Ick Soo Kim ^{1,*} 

¹ Nano Fusion Technology Research Group, Institute for Fiber Engineering (IFES), Interdisciplinary Cluster for Cutting Edge Research (ICCER), Shinshu University, Tokida 3-15-1, Ueda 386-8567, Nagano, Japan; sanamalik269@gmail.com (S.U.)

² Institute of Inorganic Chemistry I, Helmholtz Institute of Ulm (HIU), Ulm University, Helmholtzstrasse 11, 89081 Ulm, Baden Württemberg, Germany

³ Department of Chemistry, The University of Lahore, Sargodha Campus, Sargodha 40100, Pakistan

⁴ Faculty of Textile Science and Technology, Shinshu University, Ueda 386-8567, Nagano, Japan

⁵ School of Textile and Clothing, Nantong University, Nantong 226019, China

⁶ Consumer Product Division, Korea Conformity Laboratories, Seoul 08503, Republic of Korea

* Correspondence: kim@shinshu-u.ac.jp

† These authors contributed equally to this work.

Abstract: Water pollution is increasing with rapidly growing industries and world population, which is very harmful for marine life and humans as well. This research has been conducted to introduce novel material with advanced techniques for the effective removal of heavy metals from wastewater. Successful nanofiber membranes have been developed with hemp charcoal (HC) and polyacrylonitrile (PAN), which can remove heavy metals from water efficiently in less time. The nanofiber membranes showed good adsorption capacity for heavy metal ions along with good thermal and mechanical stability. Electrospun nanofibers of HC and PAN were assessed for adsorption capacity by soaking them in metallic suspensions of known concentration for a specific period of time. Nickel, cobalt, and copper metals were selected to assess the adsorption capacity of nanofibrous webs. It was observed that HC played a vital role in removing metal ions from wastewater with an excellent efficiency. The adsorption capacity for nickel, cobalt, and copper was 54 mg/g, 87 mg/g, and 96 mg/g, respectively.

Keywords: hemp charcoal; wastewater; heavy metals; electrospinning; sustainability



Citation: Ullah, S.; Ohsawa, O.; Ishaq, T.; Hashmi, M.; Sarwar, M.N.; Zhu, C.; Ge, Y.; Jang, Y.; Kim, I.S.

Fabrication of Novel Hemp Charcoal Nanofiber Membrane for Effectual Adsorption of Heavy Metal Ions from Wastewater. *Sustainability* **2023**, *15*, 9365. <https://doi.org/10.3390/su15129365>

Academic Editor: Francesco Ferella

Received: 12 April 2023

Revised: 7 June 2023

Accepted: 8 June 2023

Published: 9 June 2023



Copyright: © 2023 by the authors. Licensee MDPI, Basel, Switzerland. This article is an open access article distributed under the terms and conditions of the Creative Commons Attribution (CC BY) license (<https://creativecommons.org/licenses/by/4.0/>).

1. Introduction

With the increase in population and the development of industrialization, there is a growing need of clean and green sources to fulfill the various needs of mankind, especially water bodies which are one of the most significant resources and have political, economic, environmental and social impacts on the whole world. The main sources of water bodies comprise ground water, reservoirs, lakes canals, rainwater harvesting, atmospheric water production, sea water and fog collection [1]. The growing industries provided a lot of benefits to humanity but caused a lot of pollution as well by releasing noxious substances to the environment [2,3]. Heavy metals are one of those toxics released by the industries into the water bodies and this heavy metal toxicity causes serious environmental pollution. Heavy metals can directly affect human health [4,5], for example, copper (Cu), which is an essential nutrient for the effective metabolism of animals, in excess may lead to various damaging effects such as convulsions, cramps, vomiting and sometimes death. For instance, divalent copper (Cu II) poisoning can cause dramatization, keratinization, and the itching of feet and hands [6]. Cobalt (Co) is another heavy metal which can be accumulated and transmitted via food chains and is noxious to human health. Its usage can cause low blood pressure, gene mutation and bone defects. Furthermore, nickel (Ni)

poisoning can cause headache, dizziness, nausea, pain or tightness in the chest, heavy weakness, breathing issues, cyanosis and dry cough [1]. High Ni consumption leads to the cancer of the nose, lungs and bones [7]. Thus, all heavy metals can lead to serious and harmful ecological impacts [8] which may cause all kinds of health disorders [9]. In the present era, many techniques such as membrane separations, electrolytic processes, ion-exchange processes, chemical precipitation and adsorption methods have been used to remove heavy metals [10]. However, these techniques are not satisfactory in removing these metals in an efficient way since a few of them require high energy and high cost while others are noxious, for instance, membrane separation and electrolytic methods' demand for high energy utilization are costly while ion-exchange techniques and chemical precipitation cause secondary pollution and produce much poisonous and non-degradable chemical sludge which is also hazardous.

On the other hand, the adsorption technique proves to be a more promising tactic [11] owing to its high efficiency, ease, simplicity and low cost [12,13]. Moreover, the adsorption of small molecules on the surface of a solid support is effective for secondary pollution control. Although various solid supports, such as metal nanoparticles [14], metal-organic frameworks [15] or other metal nanocomposites [16], activated charcoal [17], graphene [14], silica [18], natural materials [19] macromolecules and other polymers [20,21] have been used successfully to treat heavy metals but with various obstacles and limitations. For instance, the pores of various porous materials are not able to capture many metallic ions with high efficiency, while carbonaceous materials such as graphene are very costly and it is difficult to recycle them which make them more expensive. Furthermore, silica gel modified with various functional groups does not show any considerable efficiency for heavy metal removal since these functional groups reveal very low modifications [17]. Hence, designing a novel adsorptive material with super adsorptive performance for commercial application is still a major concern. Phenylenediamine and its sulfonate have also been used as adsorbents for heavy metals [22]. Not only nanofibers and nanomaterials have been used for adsorption, but there have been reports where olive mill wastewater has been treated using different reactors as well [23,24].

Recently, the fabrication of efficient adsorbents with various morphologies such as nanofibers [25], nano-beads and nanocomposites has been applied in heavy metal removal. Nanostructured materials with a fibrous morphology have become an ideal adsorbent owing to their high permeability, high porosity and larger surface area with a large variety of functional groups, which leads to high adsorption aptitude. Furthermore, electrospinning is an economical, versatile and relatively simple technique for the fabrication of nanofibers [26] with ultrafine dimensions ranging from 10^{-9} to 10^{-6} m and are well renowned for wastewater treatment being efficient adsorbents [27]. Electrospun nanofiber mats are highly porous with an interconnected pore structure which enables them to act as efficient adsorbents for heavy metal removal [28] owing to their high binding potential for heavy metal ions [29]. Additionally, they can be tailored with various functional moieties to enhance their water treatment ability and thus have become the hotspot of recent advances in water treatment technology [30]. Apart from wastewater treatment, electrospun nanofibers have a broad range of applications due to their unique structure and higher surface areas [31].

In recent years, the fabrication of efficient adsorbents utilizing polyacrylonitrile fiber (PAN) as a carrier and supportive material has acquired great attention [30]. PAN is an extensively used material at the commercial level and has seen uses in ultrafiltration [32], microfiltration [33] and desalination [12] due to its low cost, easy availability [34], higher mechanical strength [35], excellent flexibility and eco-benign nature [34]. Furthermore, PAN is rich in nitrile groups that can be conveniently transformed into amide, amidoxime and carboxyl by various grafting mechanisms [17]. Moreover, it can be efficiently woven into distinct and novel shapes for usage in continuous-flow processes. Many PAN-supported materials have been designed for the effective removal of heavy metal ions [36]. However, the absorption capacity of pristine PAN membranes is very low, which limits their

application in wastewater treatment. To meet this challenge, various endeavors have tried modifying its surface [12]. For instance, Sheng et al. [37] thio-functionalized the surface of PAN for the enhanced absorption of Cd^{2+} and Hg^{2+} . Conversely, there was no satisfactory performance for the removal of other heavy metals. Gang et al. [17] designed a novel and highly selective chelating fiber loaded with a bis(2-pyridylmethyl) amino group on the surface of PAN. The designed membrane could be conveniently recycled and reused for metallic ion absorption. Pimolpun et al. [27,38] immobilized the imine groups on the surface of PAN using NaOH (aqueous/ethanolic solution) to modify the surface of PAN fiber with an imine-conjugated sequence which enhanced the chelation rate of metal ions for the effective removal of these metals. However, the fabrication technique of these membranes was very costly and complicated [12].

At present, there has been a tremendous amount of publications (from ancient times to the present) devoted to the applications of charcoal as a good adsorbent for various applications including water purification [39], metal precipitation [40], adsorption of various gases [41], removal of heavy metal ions [42] and aqueous organic species [39]. In a study, it was reported that charcoal utilization is in fact a conservable energy route for environmental protection. Charcoal installment in a room decreases room humidity, air polluting substances and offensive odor. Hence, it is a novel material for sustaining a good quality life on Earth [43]. Owing to a large number of benefits offered by charcoal, it has been applied in pristine form [44] as well as in conjunction with other materials for the cleaning of water such as chitosan/charcoal [42] and acrylonitrile-butadiene-styrene/charcoal [45], but there is no report about the fabrication and utilization of hemp charcoal (HC)-modified PAN membranes for heavy metal removal to date to the best of our knowledge.

Herein, we reported the fabrication of a highly efficient and novel hybrid immobilization of hemp charcoal (HC) on pristine PAN surface via the electrospinning technique and the adsorption capacities of nickel, cobalt, and copper were analyzed to evaluate the potential of hemp charcoal/PAN (HC/PAN) nanofibers as a suitable material for wastewater treatment. The characterization of the fabricated materials was done via wide-angle X-ray diffraction (WAXRD), Fourier transform infrared spectroscopy (FTIR), and scanning electron microscope (SEM-EDX), while mechanical properties were studied via thermogravimetric analysis (TGA), TDA and TDC. The adsorption capacity of the HC/PAN with varying concentration of HC was analyzed via inductively coupled plasma (ICP).

2. Experimental Work

2.1. Reagents

PAN in white powder form having an average molecular weight of 150,000 was purchased from the Sigma-Aldrich Corporation (Saint Louis, MO 63103, USA). *N,N*-Dimethylformamide (DMF) was purchased from FUJIFILM Wako Pure Chemical Corporation (Osaka, Japan). Hemp charcoal was the courtesy of Yashu Asazumi Lab, Japan. Distilled water was used from the laboratory.

2.2. Method

The solution of PAN (8% by weight) was made in DMF. The solution was stirred at 60 °C for 8 h, and 3%, 5% and 10% of hemp charcoal was added in the solution while stirring. After that, the solution was kept for sonication for 4 h. The sonicated solution was prepared for electrospinning for nanofiber fabrication. A Syringe capacity of 20 mL and a nozzle with a diameter of 0.5 mm was used for electrospinning. Voltage was kept fixed at 15 kV, the distance between nozzle tip and nanofiber collector drum was kept at 14 cm, and the flow rate of the solution was 0.5 mL/h. Electrospinning conditions were kept the same for all samples.

3. Results and Discussion

3.1. Morphological Characteristics

Morphological analysis of the fabricated nanofibers was done via a scanning electron microscope (SEM) (JSM-5300, 20 kV, JEOL Ltd., Tokyo, Japan). The surface morphology of the designed binary nanofibrous mats is shown in Figure 1. Thin, long and smooth fibers with uniform diameter were observed with a fiber length of a few micrometers and a fiber diameter of a few nanometers for 3%HC/PAN. These nanofibers were similar to the already reported results of pristine PAN in regard to their morphology [46,47] which meant that HC with a concentration of 3% did not significantly affect the fibrous shape and dimensions. In the case of 5%HC/PAN, the diameter of PAN fibers was increased and the uniformity of these nanofibers was decreased due to bead formation, which further enhanced the diameter (at the point of bead formation). This increase in diameter and bead formation indicated that the surface area of the PAN was reduced with an increase in hemp charcoal on the surface of nanofibers. This may lead to the conclusion that there is weak physical bonding between PAN and HC and, for that reason, HC will be stable on the surface of nanofibers. Surface roughness was seen with the further enhancement of charcoal sensitization on the PAN mats in 10%HC/PAN and thus reduced the metal adsorption capacity of the designed hybrid. It showed that the enhanced amount of HC destroys the surface smoothness of the PAN which is responsible for its higher adsorption capacity and, thus, a higher HC concentration decreases the supremacy of the PAN adsorbent for the effective removal of heavy metal ions.

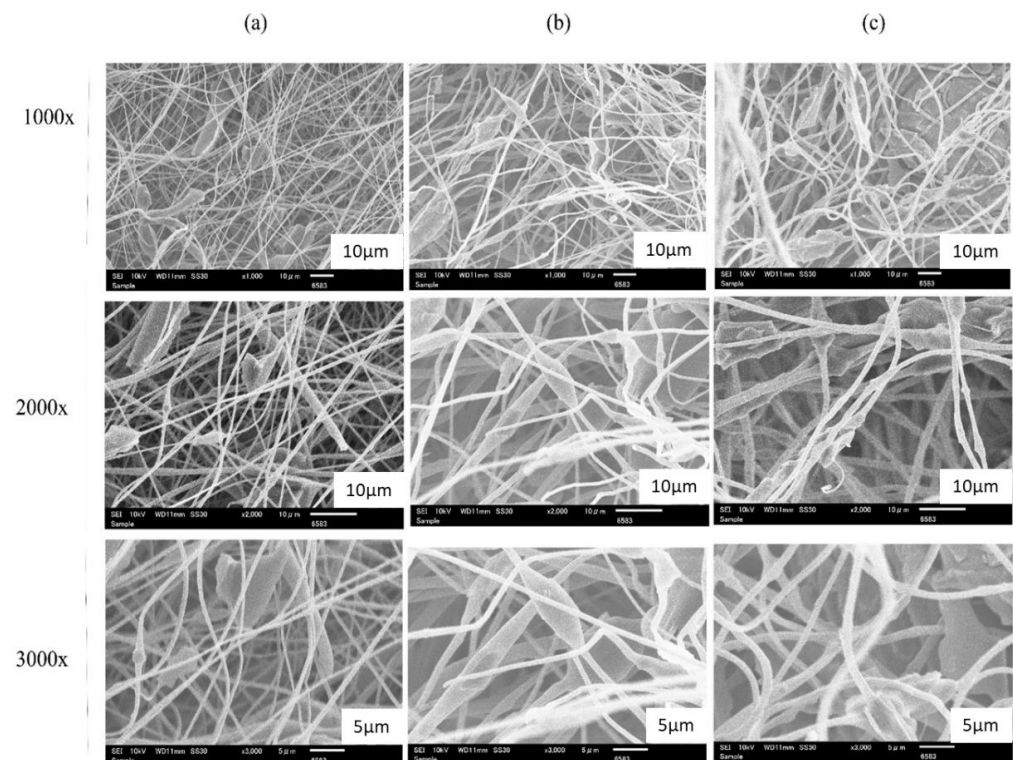


Figure 1. Morphological properties of (a) 3% HC/PAN, (b) 5% HC/PAN, and (c) 10% HC/PAN at different resolutions.

Diameter Distribution

The average diameter of the nanofibers was calculated by ImageJ software (IJ153) from readings of 50 random nanofibers from each sample. It was observed that the diameters of the nanofibers was slightly increased with increased hemp charcoal loading. For samples having 3% HC, the average diameter was 205 nm, while the diameter was 212 nm and 235 nm for 5% HC and 10% HC, respectively. Figure 2 represents the diameter distribution of 3% HC/PAN, 5% HC/PAN, and 10% HC/PAN nanofibers.

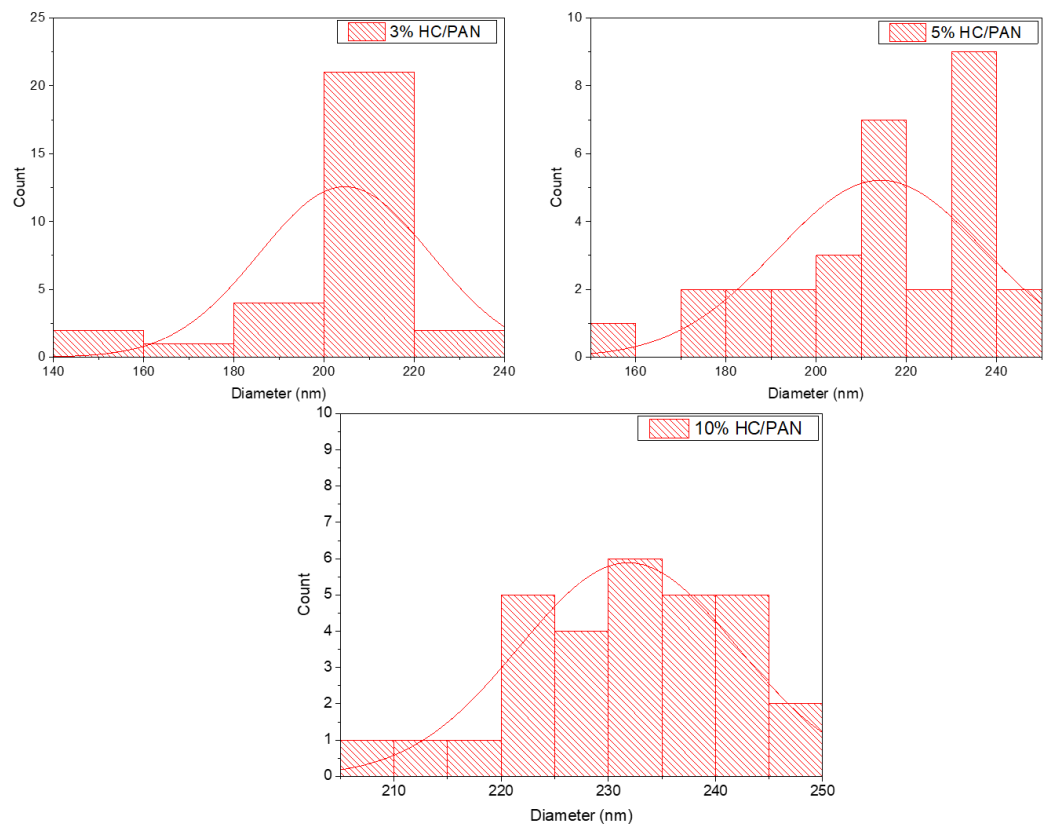


Figure 2. Diameter distribution of 3% HC/PAN, 5% HC/PAN, and 10% HC/PAN nanofibers.

3.2. EDX Composition Analysis

To confirm the charcoal sensitization of PAN, EDX analysis was performed (Figure 3). It was revealed that C and K peaks were present in all the fabricated samples (since the charcoal used was activated charcoal). Furthermore, higher counts were observed in the samples having higher concentrations of HC in the PAN mats. These values are not the exact presentation of HC functionalization on the PAN mat, but these values show a direct relation of HC with PAN samples. The exact amount of HC on the PAN mats is depicted in Table 1.

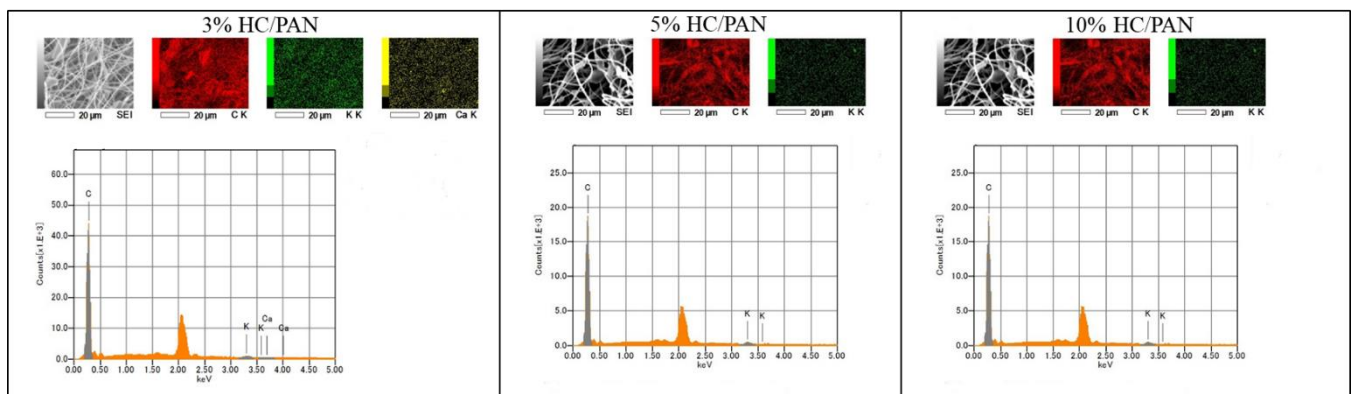


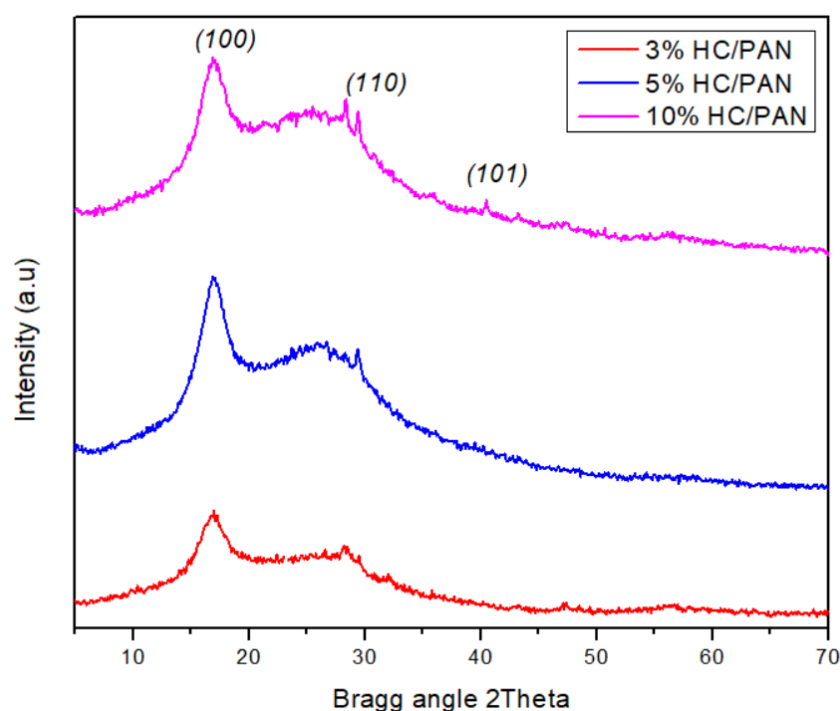
Figure 3. EDX of PAN nanofibers with 3%, 5%, and 10% hemp charcoal.

Table 1. Ratio of varying amount of HC and PAN in all the three designed hybrids, i.e., 3% HC/PAN, 5% HC/PAN and 10% HC/PAN.

Sr. No	Sample Code	Weight Proportions
1	3% HC/PAN	3% HC
2	5% HC/PAN	5% HC
3	10% HC/PAN	10% HC

3.3. XRD Analysis

Crystallographic studies were performed by wide-angle X-ray diffraction (WAXRD) using the Rotaflex RT300 mA, Rigaku, Osaka, Japan with an angular angle of $5 \leq 2\theta \leq 70^\circ$. Nickel-filtered Cu-K α rays were used as an X-ray source with an operating current of 300 mA at a temperature of 25 °C. Figure 4 validates the XRD spectrum of PAN with a varying concentration of HC, i.e., 3%, 5% and 10% HC. In the case of the 3% and 5% HC/PAN material, there was no characteristic peak corresponding to HC owing to its very low concentration, while the typical peaks of PAN were witnessed in the XRD plot for pristine PAN, indicating that HC insertion did not alter the crystallographic arrangement of PAN which is responsible for its mechanical strength and flexibility. There are two distinctive diffraction signals: one peak with a relatively high intensity at a 2θ value of 16.5° and the other with a lower intensity peak at 29.0° , indicating the ordered crystalline structure of linear macromolecules of PAN, as depicted in Figure 4. The intense signal at 16.5° is indexed as (100) and connected to molecular chain spacing, while the peak with low-angle diffraction at (110) is ascribed to parallel molecular spaces among the various macromolecular fibers. Furthermore, the presence of the wide diffuse reflection region between the two diffracting signals of 29° and 16.5° reveals the homogeneity of the disordered phase in the PAN material [48]. In 10% HC/PAN, an additional peak appears at 44° in the XRD plot, which is indexed as (101), indicating the presence of graphitic layers of the charcoal [49], i.e., HC, which reveals that the PAN was successfully functionalized with HC.

**Figure 4.** Crystallographic XRD pattern of 3% HC/PAN, 5% HC/PAN and 10% HC/PAN hybrids.

3.4. FTIR Studies

FTIR (ATR Prestige-21, Shimadzu, Japan) spectra with a wave range from 600 cm^{-1} to 4000 cm^{-1} were used for functional group determination and chemical analysis (Figure 5). The two sharper peaks were present, one at 2244 cm^{-1} which may be credited to $\text{C}\equiv\text{N}$ stretching and the other at 1451 cm^{-1} which was ascribed to $\text{C}-\text{H}$ bending. Furthermore, the absorption bands at 2933 cm^{-1} and 1617.9 cm^{-1} were ascribed to the stretching modes of $\text{C}-\text{H}$ and $\text{C}=\text{O}$ respectively. All these four absorption bands are the characteristic bands of PAN which verifies its presence in the fabricated hybrid [50]. Additionally, few peaks of the lower intensity were observed at 880 cm^{-1} and in the range of $2800\text{--}3000\text{ cm}^{-1}$ in the FTIR spectrum. Among these bands, the peak at 880 cm^{-1} was ascribed to the outer aromatic vibrational mode while bands present in the $2800\text{--}3000\text{ cm}^{-1}$ region revealed the presence of CH , CH_2 and CH_3 groups, and all these peaks justify the successful immobilization of HC on the PAN surface, which in turn enhanced its surface area for the high absorption rate of heavy metal removal [45].

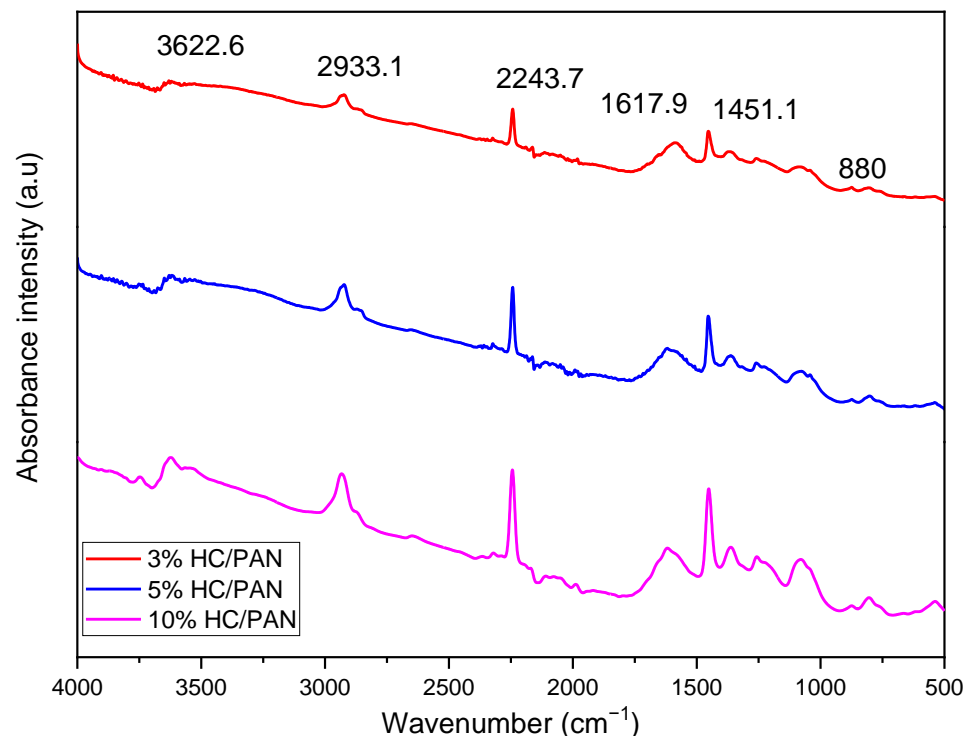


Figure 5. FTIR spectra of 3% HC/PAN, 5% HC/PAN and 10% HC/PAN binary hybrid mats.

3.5. Mechanical Properties

Mechanical characteristics of the designed hybrid nanofibers were evaluated by the Universal Testing Machine (UTM), (Tensilon RTC 250A, A&D Company Ltd., Tokyo, Japan) by preparing five specimens for each nanofibrous sample following the ISO 13,634 testing standard and the analysis was done at room temperature under a crosshead speed of 5 mm/min . Mechanical assets, i.e., tensile stress, tensile strain and Young's modulus, were calculated from UTM data by the following equations, respectively:

$$\sigma = \frac{F}{A} \quad (1)$$

$$\varepsilon = \frac{\Delta l}{l} \quad (2)$$

$$E = \frac{\sigma}{\varepsilon} \quad (3)$$

where σ denotes stress, F is the force applied, A is the cross-sectional area of the specimen, ϵ denotes the strain, Δl is the change in length, l is the original length and E corresponds to Young's modulus, of the specimen.

All the UTM data have been arranged in Table 2, while the stress–strain plot is shown in Figure 6. From Figure 6, it is revealed that 3% HC/PAN shows the highest value of tensile strength (2.3 MPa) among all three of the fabricated hybrids while 10% HC/PAN shows the lowest value of 1.17 MPa. This indicates that HC sensitization does nothing to reinforce the strength of PAN mats; rather, the HC powder decreased tensile strength. The values of the elastic modulus for the designed hybrids with charcoal sensitization of PAN were also decreased with an increase in concentration of HC. Furthermore, elongation at the break point was also decreased for the fabricated binary hybrid adsorbents, as shown in Table 2.

Table 2. Mechanical properties of 3% HC/PAN, 5% HC/PAN, and 10% HC/PAN.

Properties	3% HC/PAN	5% HC/PAN	10% HC/PAN
Elastic modulus	0.1375	0.01753	0.0895
Elongation at break	18.19	15.1	16.4
Tensile strength	2.3 MPa	2.20 MPa	1.17 MPa

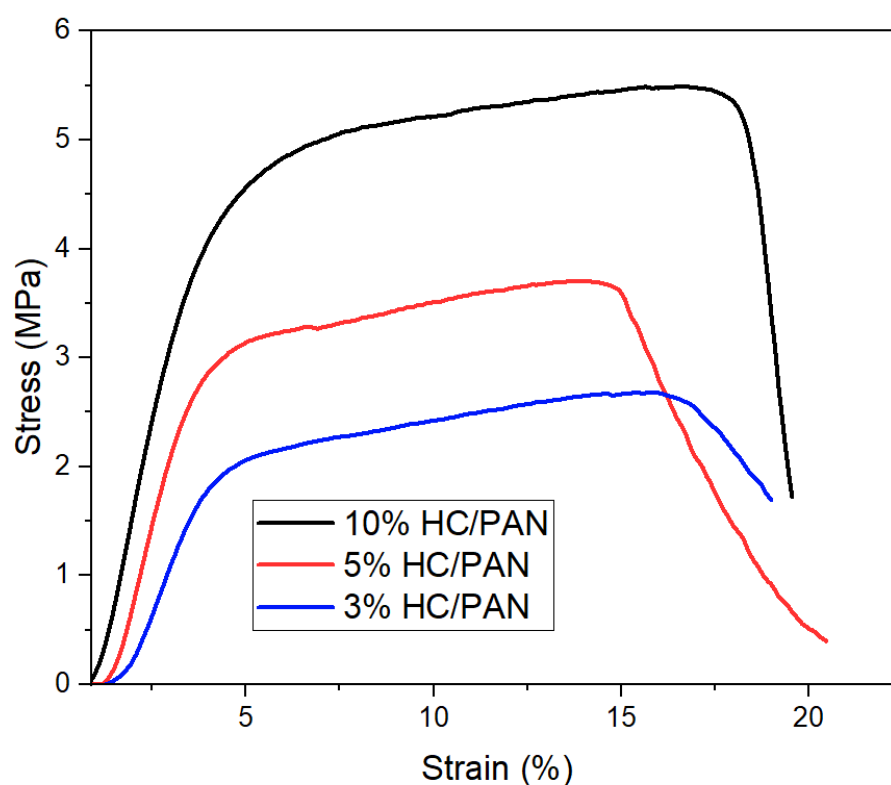


Figure 6. Stress–strain plot of 3% HC/PAN, 5% HC/PAN and 10% HC/PAN binary hybrid mats.

3.6. Thermogravimetric Analysis (TGA)

The evaluation of thermal degradation was carried out via a thermogravimetric analyzer (Thermo-plus TG 8120, Rigaku Corporation, Osaka, Japan). TGA was executed at an ambient atmospheric condition in the static mode at a temperature range of 25–500 °C (ramping rate of 10 °C/min) for all the fabricated samples. The thermal curve between mass loss (%) and the temperature of electrospun PAN fibers incorporated with varying concentrations of hemp charcoal, i.e., 3%, 5% and 10% HC, is depicted in Figure 7. The variation in weight of 3% HC/PAN, 5% HC/PAN and 10% HC/PAN with temperature

validates the various stages of thermal breakdown, mass loss, threshold temperatures and thermal stability. The degradation in the TGA curve can also be attributed to the production of nitrogenous gases by the process of dehydrogenation, cyclization or the reactions occurring on the surface of the PAN mats [51]. It was revealed that with HC functionalization, the thermal decomposition of PAN was decreased, which was credited to the enhanced cyclization of PAN mats with HC insertion [48]. The first part of the TGA curve usually represents that removal of water (up to 100 °C) and the loss of volatile compounds, i.e., when moisture or impurities with a low boiling point appeared. The second part of the thermal plot represents the degradation of the PAN while the third part shows the combustion of the PAN. It can be observed from Figure 6 that the thermal onset of 3% HC/PAN, 5% HC/PAN and 10% HC/PAN was observed at 300–320 °C as the concentration increased. This shows that with an increase in the percentage of HC, the thermal stability of the PAN also increases; thus, HC reinforced the thermal stability of PAN matrix. The thermogram shows that the residual amounts of 3% HC/PAN, 5% HC/PAN and 10% HC/PAN were 0.19%, 0.48 and 0.36%, respectively, which depicted that all the designed PAN hybrids were decomposed within the range of 50–600 °C.

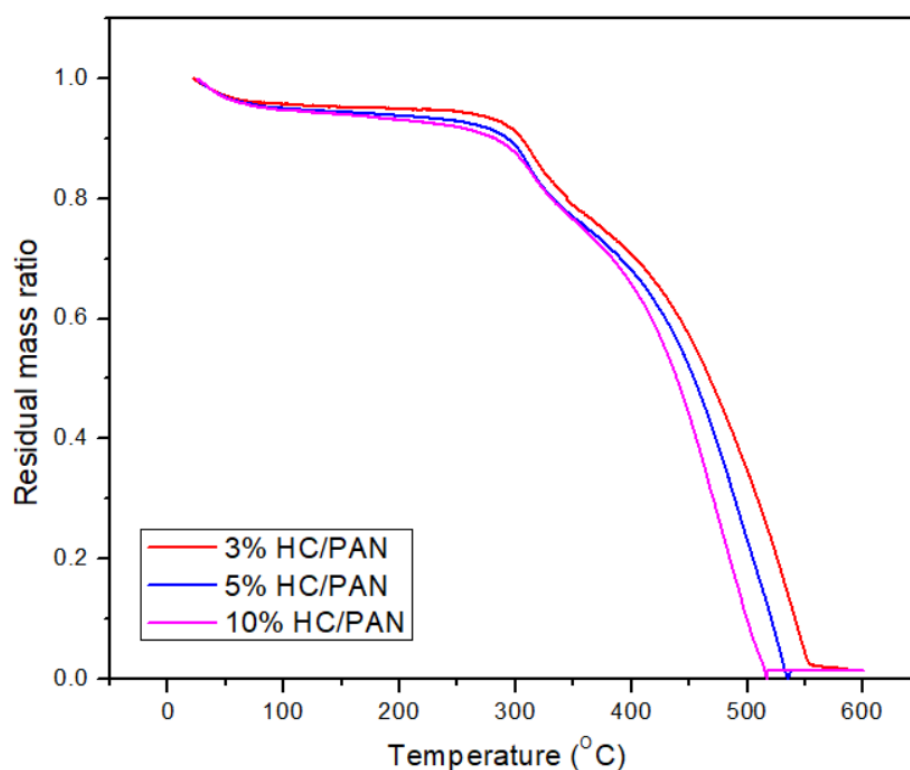


Figure 7. Thermal degradation analysis (TGA plot) of 3% HC/PAN, 5% HC/PAN and 10% HC/PAN binary hybrid mats.

3.7. Differential Thermal Gravimetric Curve (DTG)

The derivative thermogravimetric (DTG) curves of 3% HC/PAN, 5% HC/PAN and 10% HC/PAN binary hybrids are shown in Figure 8. The DTG curve demonstrates that the nanofibers with 3% and 10% HC had lower weight loss as the temperature increased, which was consistent with the TGA results. The temperature of weight loss for 5% HC/PAN was 537.5 °C, which was higher than the 3% HC/PAN and 10% HC/PAN. The DTA results show the exothermic peak at 541 °C, which corresponds to weight reduction in the range of 200–600 °C, as shown in Figure 8 which also indicated that PANF with 5% HC could form the ladder structure, which promotes the ionic mechanism of the cyclization reaction [52].

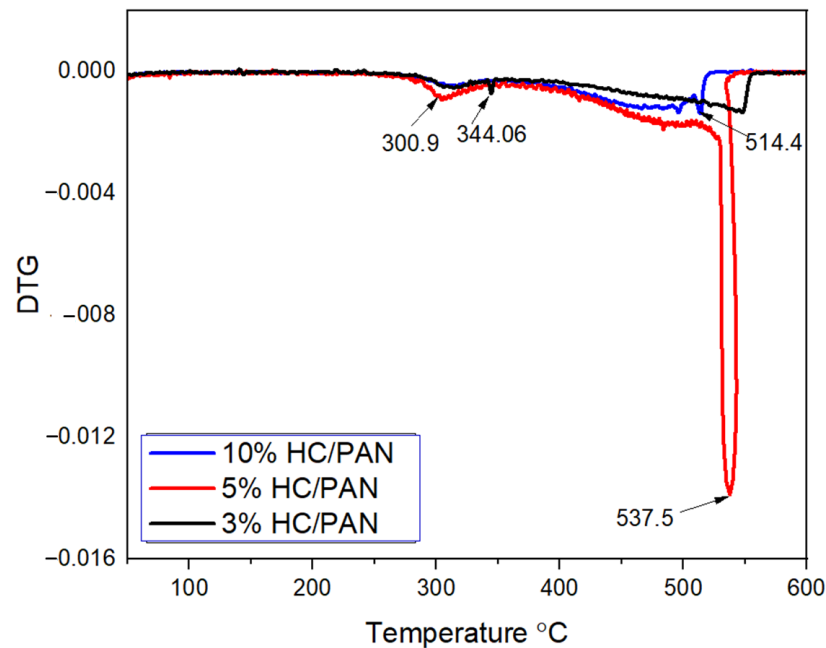


Figure 8. Differential thermogravimetric analysis of PAN nanocomposite fibers with different hemp charcoal loadings: 3% HC/PAN, 5% HC/PAN and 10% HC/PAN.

3.8. Differential Thermal Analysis (DTA)

The differential thermal analysis (DTA) curves of 3% HC/PAN, 5% HC/PAN and 10% HC/PAN are shown in Figure 9. The initiation temperature of the DTA exothermic peak in PAN nanofiber with 3%, 5% and 10% HC/PAN was at 220 °C with a maximum peak at 306.2 °C due to the thermal polymerization of nitrile groups. The sharp DTA peak of 5% HC/PAN at 541.9 °C indicated the exothermic reaction which corresponds to widespread decomposition, which supports the fact that PAN has good thermal steadiness as compared with the 3% and 10% hemp charcoal concentrations, which was consistent with TGA and DTG results.

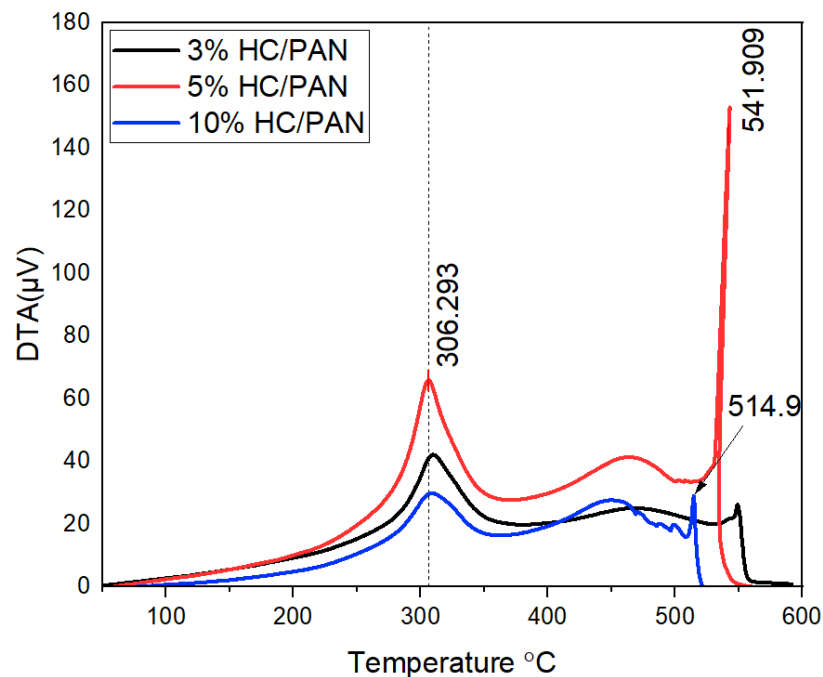


Figure 9. Differential thermo-analysis of PAN nanocomposite fibers with different hemp charcoal loadings: 3% HC/PAN, 5% HC/PAN and 10% HC/PAN.

3.9. Measurements of Adsorption Capacity

The metal adsorption potential of the PAN hybrids was evaluated via an inductively coupled plasma (ICP) atomic emission spectrometer (SHIMADZU/ICPS, 10,000 IV, Japan). The nanofiber membrane of PAN having 3%, 5% and 10% hemp charcoal (HC) was analyzed for up to 16 h for nickel, cobalt and copper ions. Standard solutions were prepared for calibration. Three standard solutions with 20 ppm, 50 ppm, and 100 ppm were prepared using nickel, cobalt, and copper salts. The coefficient factor (R^2) was calculated for all three nickel, cobalt and copper ions which was 0.9984, 0.9990, and 0.9943, respectively, as shown in Figure 10. These values of R^2 indicate the credibility of ICP analysis. Adsorption capacity was measured in mg/g. When we compared nanofiber membranes with different loadings of HC, it was observed that samples with 10% HC showed the maximum adsorption capacity for nickel and cobalt ions while 3% HC showed the minimum adsorption capacity. It can be observed from Figure 11 that nanofiber mats showed the maximum adsorption rate in the early hours and that the adsorption rate became slow after almost 5 h. The nanofiber membrane showed an excellent adsorption capacity for copper ions, which started from 95 mg/g and increased with time. In the case of copper ions, nanofiber membranes having a 10% HC ratio showed an adsorption capacity in between 3% HC and 5% HC. The nanofiber membrane with the 3% HC ratio showed the highest results, but there was a very small difference between the values of 10% HC and 3% HC nanofibers.

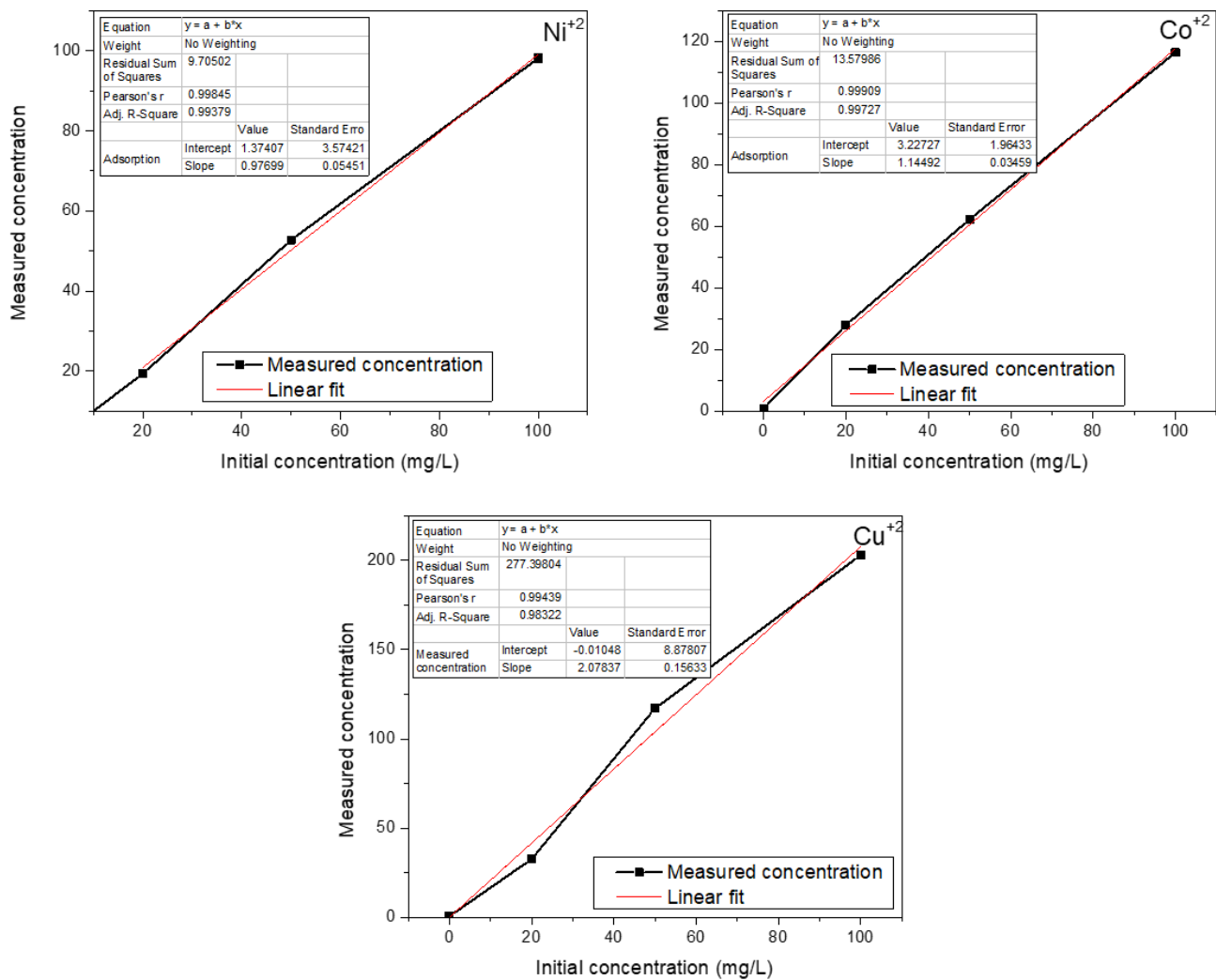


Figure 10. Coefficient factor (R^2) for nickel, cobalt, and copper standard solutions.

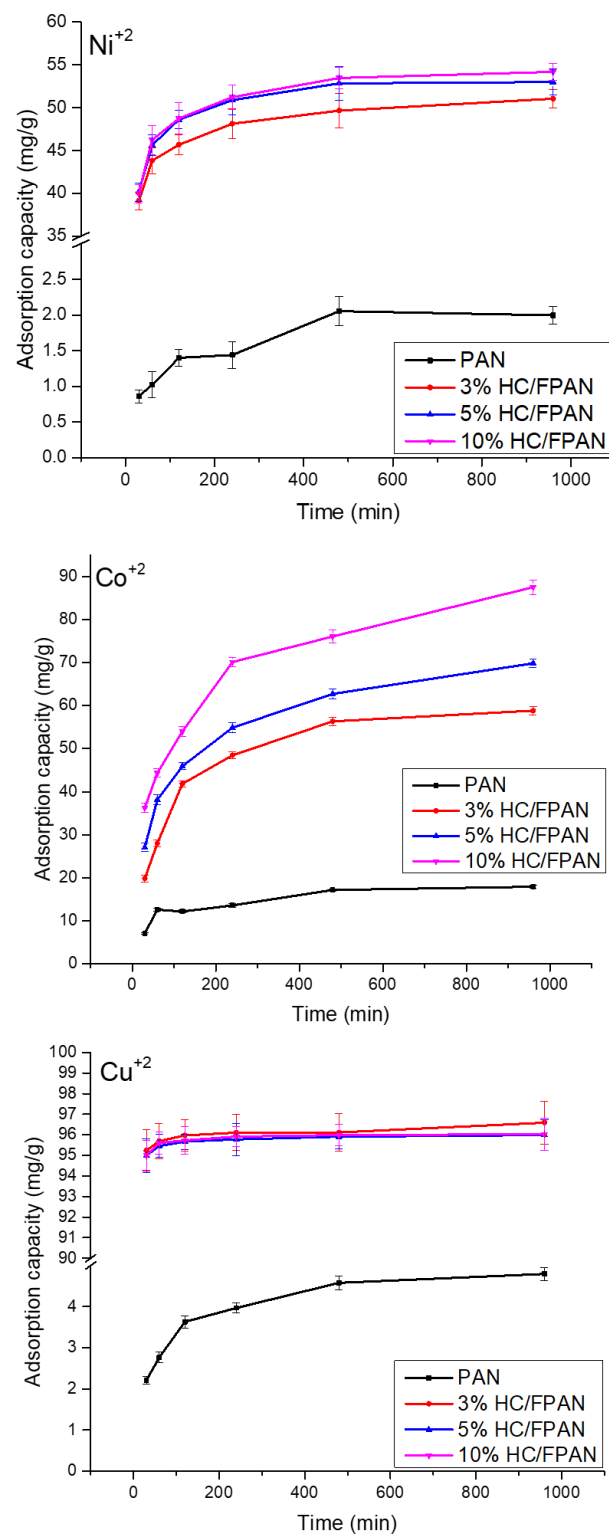


Figure 11. Removal efficiency of PAN/HC nanofibers for nickel, cobalt and copper ions.

Adsorption capacity of pure PAN nanofibers was also assessed by ICP to confirm the role of hemp charcoal in boosting the removal efficiency of heavy metals from wastewater. It was observed that PAN nanofibers did not show any significant results against nickel and copper, where the maximum adsorption capacities were 2 mg/g and 4.5 mg/g for Ni²⁺ and Cu²⁺, respectively. However, a higher adsorption capacity (17 mg/g) was recorded for cobalt.

Metal adsorption efficiency is also judged by the time to reach an equilibrium state. It was observed that in the case of Ni^{2+} , the equilibrium state occurred after 5 h; however, adsorption capacity at the time of equilibrium for 5% HC and 10% HC was 52 mg/g (with a small difference covered by a standard deviation), while for 3% HC samples it was 47 mg/g. After 5 h, the adsorption was slower and it is not recommended to continue adsorption because the efficiency will be reduced due to the extended time. The removal efficiency against cobalt was quite dependent on the concentration of HC in the PAN nanofibers. It was observed that for 3% HC, the equilibrium state occurred after 8 h; however, for 5% and 10% HC, there was a significant increment in removal efficiency even after a time period of 16 h. The maximum adsorption capacities for 3% HC, 5% HC, and 10% HC were 56 mg/g, 69 mg/g, and 87 mg/g, respectively. For 10% HC, a significant adsorption of Co^{+2} was observed. The removal of copper ions was faster than that of cobalt and nickel. The equilibrium state was attained in a short period of time (in just 90 min). The adsorption capacity was recorded at a maximum of 95 mg/g, irrespective of hemp charcoal concentration; however, without hemp charcoal, it was just 4.5 mg/g (for neat PAN nanofibers). Thus, even a low concentration of hemp charcoal has a good catching ability for copper ions, and ICP results depict this claim very well.

4. Conclusions

PAN/HC nanohybrids with three different concentrations of hemp charcoal (i.e., 3, 5, and 10% by weight) were designed successfully and reported for the very first time up to the best of our knowledge in which a simple, easy, and one-step electrospinning approach was followed. The fabricated binary nanohybrids revealed a fibrous morphology with an enhanced surface area, which is a prerequisite for the excellent adsorption of metallic ions. From SEM images, it was confirmed that nanofibers had bead formation when the concentration of HC was higher in the electrospinning solution. Mechanical strength was improved by increasing the concentration of HC; however, a slight decrease in onset temperature was observed with an increase in the HC amount in the PAN nanofibers. Nanofibrous mats were found to be thermally stable up to 300 °C. A significant increase in adsorption capacity for different heavy metals was observed with the addition of HC in PAN nanofibers. Our results reveal that PAN/HC nanohybrids are effective for metal removal purposes and pose the best adsorption capability owing to the presence of hemp charcoal. Hence, it can play a key role in helping researchers solve major environmental concerns related to increased water pollution.

Author Contributions: Conceptualization, S.U. and O.O.; data curation, T.I. and O.O., formal analysis, S.U. and Y.G.; funding acquisition, Y.J. and I.S.K.; investigation, I.S.K.; methodology, M.N.S. and S.U.; project administration, C.Z.; resources, Y.J. and I.S.K.; software, T.I. and S.U.; supervision, M.H. and I.S.K.; validation, I.S.K.; visualization, I.S.K.; writing—original draft, O.O., T.I. and S.U.; writing—review and editing, M.H. and S.U. All authors have read and agreed to the published version of the manuscript.

Funding: This work was partially supported by the EPSON International Scholarship Foundation, as well as the Japan-Egypt Research Cooperative Program between JSPS and STDF, grant number JPJSBP120206001.

Institutional Review Board Statement: Not applicable.

Informed Consent Statement: Not applicable.

Data Availability Statement: Data will be made available on request.

Acknowledgments: The authors would like to give special gratitude to Yashu Asazumi Lab, Japan and Gue Trading Co., Ltd, Japan, for providing research materials.

Conflicts of Interest: The authors declare no conflict of interest.

References

1. Uogintė, I.; Lujanienė, G.; Mažeika, K. Study of Cu(II), Co(II), Ni(II) and Pb(II) Removal from Aqueous Solutions Using Magnetic Prussian Blue Nano-Sorbent. *J. Hazard. Mater.* **2019**, *369*, 226–235. [[CrossRef](#)] [[PubMed](#)]
2. Akey, P.; Appel, I. The Limits of Limited Liability: Evidence from Industrial Pollution. *J. Finance* **2021**, *76*, 5–55. [[CrossRef](#)]
3. Soliman, N.K.; Moustafa, A.F. Industrial Solid Waste for Heavy Metals Adsorption Features and Challenges; a Review. *J. Mater. Res. Technol.* **2020**, *9*, 10235–10253. [[CrossRef](#)]
4. Fouda, A.; Hassan, S.E.D.; Abdel-Rahman, M.A.; Farag, M.M.S.; Shehal-deen, A.; Mohamed, A.A.; Alsharif, S.M.; Saied, E.; Moghanim, S.A.; Azab, M.S. Catalytic Degradation of Wastewater from the Textile and Tannery Industries by Green Synthesized Hematite (α -Fe₂O₃) and Magnesium Oxide (MgO) Nanoparticles. *Curr. Res. Biotechnol.* **2021**, *3*, 29–41. [[CrossRef](#)]
5. Fu, F.; Wang, Q. Removal of Heavy Metal Ions from Wastewaters: A Review. *J. Environ. Manag.* **2011**, *92*, 407–418. [[CrossRef](#)]
6. Huang, Y.H.; Hsueh, C.L.; Cheng, H.P.; Su, L.C.; Chen, C.Y. Thermodynamics and Kinetics of Adsorption of Cu(II) onto Waste Iron Oxide. *J. Hazard. Mater.* **2007**, *144*, 406–411. [[CrossRef](#)]
7. Hema Krishna, R.; Swamy, A.V.V.S. Physico-Chemical Key Parameters, Langmuir and Freundlich Isotherm and Lagergren Rate Constant Studies on the Removal of Divalent Nickel from the Aqueous Solutions onto Powder of Calcined Brick. *Int. J. Eng. Res. Dev.* **2012**, *4*, 29–38.
8. Naseem, K.; Huma, R.; Shahbaz, A.; Jamal, J.; Rehman, M.Z.U.; Sharif, A.; Ahmed, E.; Begum, R.; Irfan, A.; Al-Sehemi, A.G.; et al. Extraction of Heavy Metals from Aqueous Medium by Husk Biomass: Adsorption Isotherm, Kinetic and Thermodynamic Study. *Z. Phys. Chem.* **2019**, *233*, 201–223. [[CrossRef](#)]
9. Kiliç, M.; Kirbiyik, Ç.; Çepelioğullar, Ö.; Pütün, A.E. Adsorption of Heavy Metal Ions from Aqueous Solutions by Bio-Char, a by-Product of Pyrolysis. *Appl. Surf. Sci.* **2013**, *283*, 856–862. [[CrossRef](#)]
10. Zawierucha, I.; Kozłowski, C.; Malina, G. Immobilized Materials for Removal of Toxic Metal Ions from Surface/Groundwaters and Aqueous Waste Streams. *Environ. Sci. Process. Impacts* **2016**, *18*, 429–444. [[CrossRef](#)]
11. Naseem, K.; Farooqi, Z.H.; Ur Rehman, M.Z.; Ur Rehman, M.A.; Begum, R.; Huma, R.; Shahbaz, A.; Najeeb, J.; Irfan, A. A Systematic Study for Removal of Heavy Metals from Aqueous Media Using Sorghum Bicolor: An Efficient Biosorbent. *Water Sci. Technol.* **2018**, *77*, 2355–2368. [[CrossRef](#)] [[PubMed](#)]
12. Zhang, X.; Yang, S.; Yu, B.; Tan, Q.; Zhang, X.; Cong, H. Advanced Modified Polyacrylonitrile Membrane with Enhanced Adsorption Property for Heavy Metal Ions. *Sci. Rep.* **2018**, *8*, 1260. [[CrossRef](#)] [[PubMed](#)]
13. Li, X.-G.; Huang, M.-R.; Tao, T.; Ren, Z.; Zeng, J.; Yu, J.; Umeyama, T.; Ohara, T.; Imahori, H. Highly Cost-Efficient Sorption and Desorption of Mercury Ions onto Regenerable Poly(m-Phenylenediamine) Microspheres with Many Active Groups. *Chem. Eng. J.* **2020**, *391*, 123515. [[CrossRef](#)]
14. Cortés-Arriagada, D.; Toro-Labbé, A. Improving As(III) Adsorption on Graphene Based Surfaces: Impact of Chemical Doping. *Phys. Chem. Chem. Phys.* **2015**, *17*, 12056–12064. [[CrossRef](#)] [[PubMed](#)]
15. Liang, L.; Chen, Q.; Jiang, F.; Yuan, D.; Qian, J.; Lv, G.; Xue, H.; Liu, L.; Jiang, H.L.; Hong, M. In Situ Large-Scale Construction of Sulfur-Functionalized Metal-Organic Framework and Its Efficient Removal of Hg(II) from Water. *J. Mater. Chem. A* **2016**, *4*, 15370–15374. [[CrossRef](#)]
16. Hughes, D.L.; Afsar, A.; Harwood, L.M.; Jiang, T.; Laventine, D.M.; Shaw, L.J.; Hodson, M.E. Adsorption of Pb and Zn from Binary Metal Solutions and in the Presence of Dissolved Organic Carbon by DTPA-Functionalised, Silica-Coated Magnetic Nanoparticles. *Chemosphere* **2017**, *183*, 519–527. [[CrossRef](#)]
17. Xu, G.; Wang, L.; Xie, Y.; Tao, M.; Zhang, W. Highly Selective and Efficient Adsorption of Hg²⁺ by a Recyclable Aminophosphonic Acid Functionalized Polyacrylonitrile Fiber. *J. Hazard. Mater.* **2018**, *344*, 679–688. [[CrossRef](#)]
18. Roosen, J.; Van Roosendaal, S.; Borra, C.R.; Van Gerven, T.; Mullens, S.; Binnemans, K. Recovery of Scandium from Leachates of Greek Bauxite Residue by Adsorption on Functionalized Chitosan–Silica Hybrid Materials. *Green Chem.* **2016**, *18*, 2005–2013. [[CrossRef](#)]
19. Wang, J.; Li, J.; Wei, J. Adsorption Characteristics of Noble Metal Ions onto Modified Straw Bearing Amine and Thiol Groups. *J. Mater. Chem. A* **2015**, *3*, 18163–18170. [[CrossRef](#)]
20. Ullah, S.; Hashmi, M.; Hussain, N.; Ullah, A.; Sarwar, M.N.; Saito, Y.; Kim, S.H.; Kim, I.S. Stabilized Nanofibers of Polyvinyl Alcohol (PVA) Crosslinked by Unique Method for Efficient Removal of Heavy Metal Ions. *J. Water Process Eng.* **2020**, *33*, 101111. [[CrossRef](#)]
21. Hanif, Z.; Lee, S.; Hussain Qasim, G.; Ardiningsih, I.; Kim, J.-A.; Seon, J.; Han, S.; Hong, S.; Yoon, M.-H. Polypyrrole Multilayer-Laminated Cellulose for Large-Scale Repeatable Mercury Ion Removal. *J. Mater. Chem. A* **2016**, *4*, 12425–12433. [[CrossRef](#)]
22. Huang, M.R.; Lu, H.J.; Li, X.G. Synthesis and Strong Heavy-Metal Ion Sorption of Copolymer Microparticles from Phenylenediamine and Its Sulfonate. *J. Mater. Chem.* **2012**, *22*, 17685–17699. [[CrossRef](#)]
23. Rocha, C.; Soria, M.A.; Madeira, L.M. Olive Mill Wastewater Valorization through Steam Reforming Using Hybrid Multifunctional Reactors for High-Purity H₂ Production. *Chem. Eng. J.* **2022**, *430*, 132651. [[CrossRef](#)]
24. Tosti, S.; Accetta, C.; Fabbri, M.; Sansovini, M.; Pontoni, L. Reforming of Olive Mill Wastewater through a Pd-Membrane Reactor. *Int. J. Hydrogen Energy* **2013**, *38*, 10252–10259. [[CrossRef](#)]
25. Hashmi, M.; Ullah, S.; Ullah, A.; Khan, M.Q.; Hussain, N.; Khatri, M.; Bie, X.; Lee, J.; Kim, I.S. An Optimistic Approach “from Hydrophobic to Super Hydrophilic Nanofibers” for Enhanced Absorption Properties. *Polym. Test.* **2020**, *90*, 106683. [[CrossRef](#)]

26. Morillo Martín, D.; Faccini, M.; García, M.A.; Amantia, D. Highly Efficient Removal of Heavy Metal Ions from Polluted Water Using Ion-Selective Polyacrylonitrile Nanofibers. *J. Environ. Chem. Eng.* **2018**, *6*, 236–245. [[CrossRef](#)]
27. Kampalananwat, P.; Supaphol, P. Preparation and Adsorption Behavior of Aminated Electrospun Polyacrylonitrile Nanofiber Mats for Heavy Metal Ion Removal. *ACS Appl. Mater. Interfaces* **2010**, *2*, 3619–3627. [[CrossRef](#)]
28. Feng, C.; Khulbe, K.C.; Matsuura, T.; Tabe, S.; Ismail, A.F. Preparation and Characterization of Electro-Spun Nanofiber Membranes and Their Possible Applications in Water Treatment. *Sep. Purif. Technol.* **2013**, *102*, 118–135. [[CrossRef](#)]
29. Chitpong, N.; Husson, S.M. Polyacid Functionalized Cellulose Nanofiber Membranes for Removal of Heavy Metals from Impaired Waters. *J. Memb. Sci.* **2017**, *523*, 418–429. [[CrossRef](#)]
30. Zhao, R.; Li, X.; Sun, B.; Li, Y.; Li, Y.; Yang, R.; Wang, C. Branched Polyethylenimine Grafted Electrospun Polyacrylonitrile Fiber Membrane: A Novel and Effective Adsorbent for Cr(vi) Remediation in Wastewater. *J. Mater. Chem. A* **2017**, *5*, 1133–1144. [[CrossRef](#)]
31. Ullah, S.; Hashmi, M.; Lee, J.; Youk, J.H.; Kim, I.S. Recent Advances in Pre-Harvest, Post-Harvest, Intelligent, Smart, Active, and Multifunctional Food Packaging. *Fibers Polym.* **2022**, *23*, 2063–2074. [[CrossRef](#)]
32. Yang, Y.; Li, X.; Shen, L.; Wang, X.; Hsiao, B.S. Ionic Cross-Linked Poly(Acrylonitrile-Co-Acrylic Acid)/Polyacrylonitrile Thin Film Nanofibrous Composite Membrane with High Ultrafiltration Performance. *Ind. Eng. Chem. Res.* **2017**, *56*, 3077–3090. [[CrossRef](#)]
33. Zhang, J.; Xue, Q.; Pan, X.; Jin, Y.; Lu, W.; Ding, D.; Guo, Q. Graphene Oxide/Polyacrylonitrile Fiber Hierarchical-Structured Membrane for Ultra-Fast Microfiltration of Oil-Water Emulsion. *Chem. Eng. J.* **2017**, *307*, 643–649. [[CrossRef](#)]
34. Almasian, A.; Jalali, M.L.; Fard, G.C.; Maleknia, L. Surfactant Grafted PDA-PAN Nanofiber: Optimization of Synthesis, Characterization and Oil Absorption Property. *Chem. Eng. J.* **2017**, *326*, 1232–1241. [[CrossRef](#)]
35. Sarwar, M.N.; Ullah, A.; Haider, M.K.; Hussain, N.; Ullah, S.; Hashmi, M.; Khan, M.Q.; Kim, I.S. Evaluating Antibacterial Efficacy and Biocompatibility of PAN Nanofibers Loaded with Diclofenac Sodium Salt. *Polymers* **2021**, *13*, 510. [[CrossRef](#)] [[PubMed](#)]
36. Ko, Y.G.; Chun, Y.J.; Kim, C.H.; Choi, U.S. Removal of Cu(II) and Cr(VI) Ions from Aqueous Solution Using Chelating Fiber Packed Column: Equilibrium and Kinetic Studies. *J. Hazard. Mater.* **2011**, *194*, 92–99. [[CrossRef](#)] [[PubMed](#)]
37. Deng, S.; Zhang, G.; Liang, S.; Wang, P. Microwave Assisted Preparation of Thio-Functionalized Polyacrylonitrile Fiber for the Selective and Enhanced Adsorption of Mercury and Cadmium from Water. *ACS Sustain. Chem. Eng.* **2017**, *5*, 6054–6063. [[CrossRef](#)]
38. Kampalananwat, P.; Supaphol, P. Preparation of Hydrolyzed Electrospun Polyacrylonitrile Fiber Mats as Chelating Substrates: A Case Study on Copper(II) Ions. *Ind. Eng. Chem. Res.* **2011**, *50*, 11912–11921. [[CrossRef](#)]
39. Pajooeshfar, S.P.; Saeedi, M. Adsorptive Removal of Phenol from Contaminated Water and Wastewater by Activated Carbon, Almond, and Walnut Shells Charcoal. *Water Environ. Res.* **2009**, *81*, 641–648. [[CrossRef](#)]
40. Richardson, J.C. Precipitation of Gold by Charcoal. *Nature* **1899**, *59*, 1899. [[CrossRef](#)]
41. Kingman, F. Adsorption of Hydrogen on Charcoal. *Nature* **1931**, *127*, 1931. [[CrossRef](#)]
42. Saifuddin, M.N.; Kumaran, P. Removal of Heavy Metal from Industrial Wastewater Using Chitosan Coated Oil Palm Shell Charcoal. *Electron. J. Biotechnol.* **2005**, *8*, 43–53.
43. Shibata, S.I.; Kang, B.S.; Oyabu, T.; Kimura, H.; Nanto, H. Air Purification Capability of Charcoal and Its Evaluation. *IEEJ Trans. Electr. Electron. Eng.* **2010**, *5*, 603–607. [[CrossRef](#)]
44. Firth, J.B.; Watson, F.S. The Catalytic Decomposition of Hydrogen Peroxide Solution by Animal Charcoal: The Production of Highly Active Charcoals. *Trans. Faraday Soc.* **1924**, *20*, 370–377. [[CrossRef](#)]
45. Halder, K.K.; Sachdev, V.K.; Tomar, M.; Gupta, V. EMI Shielding of ABS Composites Filled with Different Temperature-Treated Equal-Quantity Charcoals. *RSC Adv.* **2019**, *9*, 23718–23726. [[CrossRef](#)] [[PubMed](#)]
46. Ullah, S.; Hashmi, M.; Kharaghani, D.; Khan, M.Q.; Saito, Y.; Yamamoto, T.; Lee, J.; Kim, I.S. Antibacterial Properties of in Situ and Surface Functionalized Impregnation of Silver Sulfadiazine in Polyacrylonitrile Nanofiber Mats. *Int. J. Nanomed.* **2019**, *14*, 2693–2703. [[CrossRef](#)]
47. Mohammad, N.; Atassi, Y. Enhancement of Removal Efficiency of Heavy Metal Ions by Polyaniline Deposition on Electrospun Polyacrylonitrile Membranes. *Water Sci. Eng.* **2021**, *14*, 129–138. [[CrossRef](#)]
48. Qiao, M.; Kong, H.; Ding, X.; Hu, Z.; Zhang, L.; Cao, Y.; Yu, M. Study on the Changes of Structures and Properties of PAN Fibers during the Cyclic Reaction in Supercritical Carbon Dioxide. *Polymers* **2019**, *11*, 402. [[CrossRef](#)]
49. Liu, X.Y.; Huang, M.; Ma, H.L.; Zhang, Z.Q.; Gao, J.M.; Zhu, Y.L.; Han, X.J.; Guo, X.Y. Preparation of a Carbon-Based Solid Acid Catalyst by Sulfonating Activated Carbon in a Chemical Reduction Process. *Molecules* **2010**, *15*, 7188–7196. [[CrossRef](#)]
50. Feng, Q.; Wu, D.; Zhao, Y.; Wei, A.; Wei, Q.; Fong, H. Electrospun AOPAN/RC Blend Nanofiber Membrane for Efficient Removal of Heavy Metal Ions from Water. *J. Hazard. Mater.* **2018**, *344*, 819–828. [[CrossRef](#)]
51. Chauque, E.F.C.; Dlamini, L.N.; Adelodun, A.A.; Greyling, C.J.; Catherine Ngila, J. Modification of Electrospun Polyacrylonitrile Nanofibers with EDTA for the Removal of Cd and Cr Ions from Water Effluents. *Appl. Surf. Sci.* **2016**, *369*, 19–28. [[CrossRef](#)]
52. Zhang, H.; Quan, L.; Gao, A.; Tong, Y.; Shi, F. Thermal Analysis and Crystal Structure of Poly(Acrylonitrile-Co-Itaconic Acid) Copolymers Synthesized in Water. *Polymers* **2020**, *12*, 221–234. [[CrossRef](#)] [[PubMed](#)]

Disclaimer/Publisher's Note: The statements, opinions and data contained in all publications are solely those of the individual author(s) and contributor(s) and not of MDPI and/or the editor(s). MDPI and/or the editor(s) disclaim responsibility for any injury to people or property resulting from any ideas, methods, instructions or products referred to in the content.